DETERMINING ENTANGLEMENT BEHAVIOR OF BRANCHED POLYMERS

Submitted by: Ramnath Ramachandran Date: 10/26/2007

Literature review prepared in partial fulfillment of the qualifier requirements towards Ph.D. in Materials Science and Engineering at the University of Cincinnati.

Abstract

For many years, an important objective in the field of polymer science has been to develop relationships between structure and measurable physical properties of polymers. This is of practical interest because rheological properties are sensitive to certain aspects of the structure such as branching.[1, 2] Such rheological properties include the critical molecular weight *(*M_c) and the entanglement molecular weight (M_e) of a polymer. In the past, several studies[3-8] have tried to relate M_e or M_c to local structural properties such as Kuhn length (l_k) or persistence length (l_p) and the overall radius of gyration (R_g) of a polymer chain. These studies[3-8] however, were limited to their discussion of linear polymers due to the lack of data pertaining to structural properties of branched polymers. Thus currently there is a lack of understanding of a direct relationship between chain structure and physical properties of branched polymers. Owing to the sensitivity of rheological behavior to branching in polymers, there is a need to relate the structural response to branching with physical properties of the polymer.

1. Introduction

The basic idea of entanglement is that the polymer molecules in a melt are surrounded by other very long molecules that greatly restrict their motion in response to an imposed deformation. The physical properties most often associated with the entanglement

phenomena are the critical molecular weight *(M_c)* and the entanglement molecular weight (M_e). Essentially, M_c is the molecular weight at which the viscosity of the polymer starts increasing more rapidly with increasing molecular weight M, due to the presence of entanglements. M_e is defined as the molecular weight between entanglements. These properties are described in detail in the subsequent section.

The quantities such as persistence length and radius of gyration are used to describe the chain dimensions of a polymer. The persistence length (l_p) of a polymer chain is defined as the distance along the molecule at which the orientation of one segment loses its correlation with the orientation of another. In other words, if we consider tangent vectors **T**(0) and **T**(L) to the polymer at position 0 (origin of reference) and at a distance L from position 0 respectively, the persistence length is described by the auto-correlation function of the tangent vectors as

$$\left\langle \vec{T}(L)\cdot\vec{T}(0)\right\rangle = e^{-(L/l_p)} \qquad \textbf{(1)}$$

The radius of gyration (R_g) of a polymer chain is the root-mean-square distance of the mass elements of the chain from its center of gravity. Both these quantities can be measured using techniques such as small-angle scattering. Theoretical models[3-8] in the past have tried to relate l_p and R_g of linear polymers to their M_e or M_c. Three such models are discussed in this review, namely

1. Binary contacts per chain model[3]
2. Packing model[4]
3. Binary contacts per pervaded volume model[7]

It is aimed to extend the applicability of these models to branched polymer systems.

A logical step forward would then be to study the effect of branching on the chain dimensions and relate their response to the physical properties of the polymer such as M_e and M_c. Branching in polymers can be classified as regular or random branching. Regularly branched polymers include architectures such as star polymers (Fig. 1b), where the branches are obtained in a controlled manner. In randomly branched polymers (Fig. 1c), the incorporation of the branches are statistical in nature. Further, branches in polymers can also be classified as short chain (SCB) or long chain branches (LCB) as seen in Fig. 1c. Though, the choice of length for a long branch is a topic of debate, this review considers that a branch is long when it is indistinguishable from the main chain. This provides a clear distinction between short and long chain branches. Recently, it has been suggested[9] that the structural response of a chain to short chain branching is an increase in l_p. These studies are based entirely on computer simulations. Such a response has been observed experimentally[10] for the first time in short chain branched polyethylene (Fig 2a). The presence of long chain branches (LCB) is not expected to affect l_p since the number of long chain branch sites is few. But it is expected to decrease R_g since the presence of LCB's causes the molecule to occupy a volume smaller than a linear molecule of the same molecular weight. This can be seen from the schematic shown in Fig. 2b and Fig. 2c.[11] Hence, by estimating the change in l_p and R_g with branching using techniques such as small-angle scattering, and then utilizing a suitable theoretical model[7], it would be possible to relate the chain structure to the entanglement behavior in polymers.

Before discussing the three models mentioned earlier, a brief overview of the theory of entanglements is discussed here.

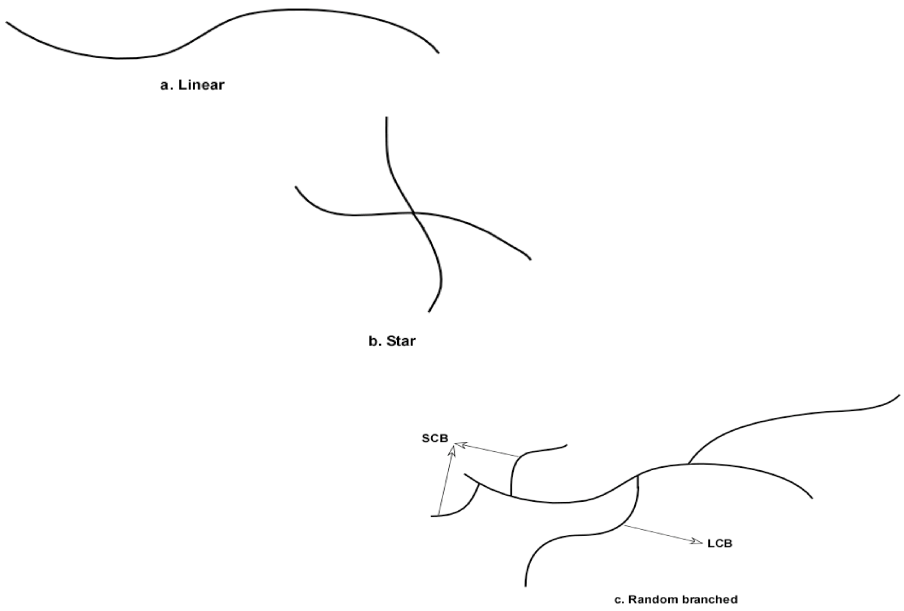

Figure 1: Schematics of (a)Linear polymer, (b) Star polymer (regularly branched) and (c) Randomly branched polymer

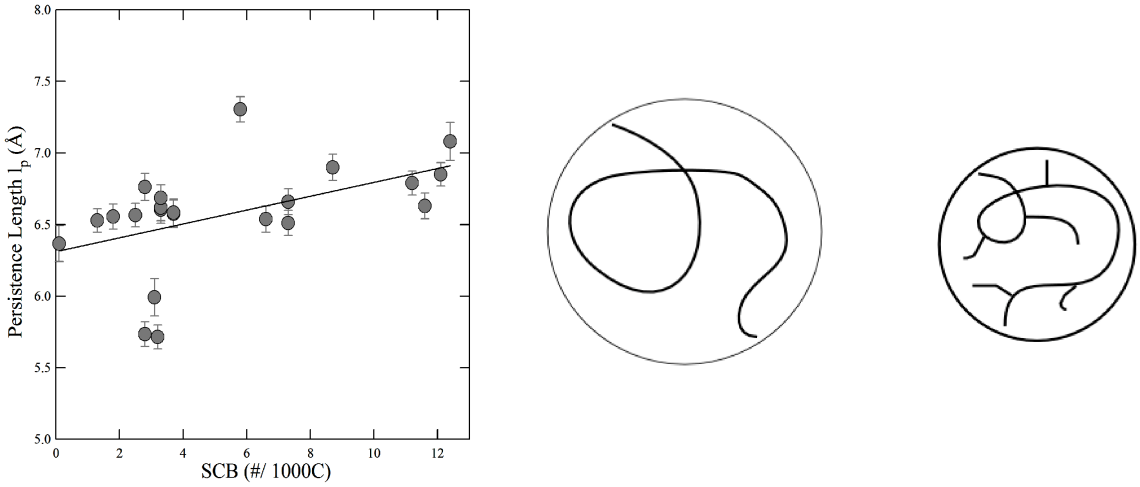

(a) **(b)** **(c)**

Figure 2: (a) Change in l_p with SCB [From ref. 10], (b) R_g of a linear polymer and (c) R_g of a branched polymer of equal molecular weight [Based on ref. 11]

2. Theory of entanglements

In the theory of linear viscoelasticity, the viscosity is independent of the shear rate. This behavior is expected at very low shear rates and the limiting low shear-rate value of viscosity is called the zero-shear viscosity η_0. Experimental observations[12] have shown that η_0 is proportional to the molecular weight M for low molecular weight polymer melts. However, η_0 of monodisperse melts increases with molecular weight much more rapidly when the molecular weight exceeds a critical value M_c known as the critical molecular weight. In fact, in the higher molecular weight region, η_0 was found[12] to be proportional to M raised to a much higher power that is usually in the neighborhood of 3.4**.** The behavior (Fig. 3a) can be summarized as

$$\eta_0 \propto M \qquad M < M_c \qquad \textbf{(2)}$$

$$\eta_0 \propto M^{3.4} \qquad M > M_c \qquad \textbf{(3)}$$

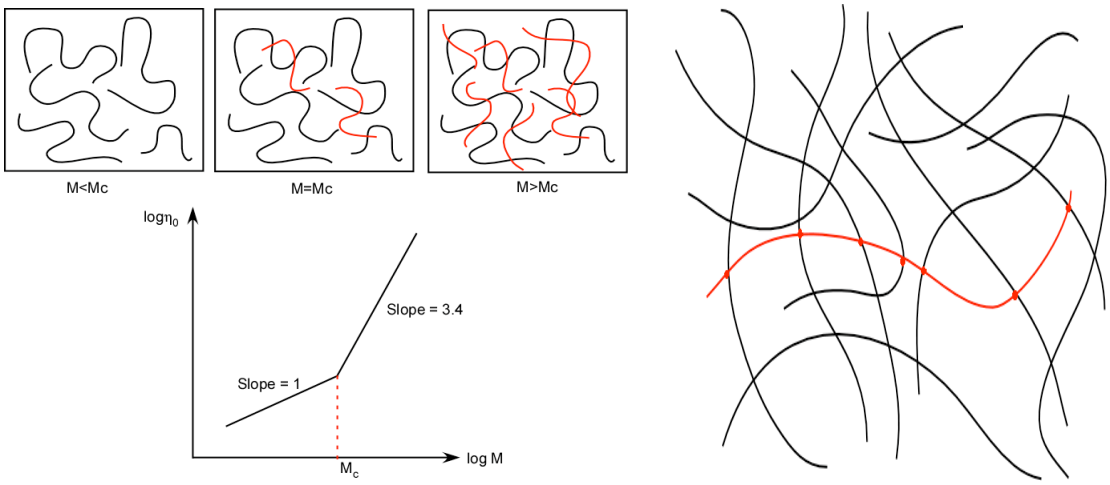

(a) **(b)**

Figure 3: (a) Variation of η_0 with molecular weight of polymer and (b) Entanglements in polymer (dots indicate site of entanglements). [Based on ref. 13]

This steeper dependence of η_0 on M is due to entanglements. In high molecular weight polymers, flexible polymer molecules are invariably entangled i.e. the motion of a polymer chain in a melt is significantly impeded by the topological constraints imposed by the neighboring chains. These constraints are referred to as entanglements. Fig. 3b shows a polymer chain entangled in a mesh of other polymer chains. As the molecular weight increases above M_c, the chain has even greater difficulty in escaping the entanglements and this leads to increase in zero shear viscosity.

The entanglement molecular weight M_e is defined as the molecular weight between entanglements. The classical theory of rubber elasticity[13] provides an expression for M_e via.

$$G_N^0 = \frac{\rho RT}{M_e} = \frac{\rho N_A kT}{M_e} \qquad \textbf{(4)}$$

where ρ is the density of the polymer melt and G_N^0 is the plateau modulus. It has also been well established experimentally that $M_c \approx 2M_e$ for a wide range of polymers.[13] To visualize the entanglement phenomena in a molecular level, a model called the tube model[13] has been described in literature.

2.1 Tube model

A highly entangled state for a polymer can be treated by an effective model named the tube model[13]. The model assumes that, the motion of such a polymer chain is essentially confined to tube-like region made of other surrounding polymers, due to steric constraints. The idea of the tube model originally was proposed in studying the problem of rubber elasticity[13]. A rubber can be described as a huge molecular network formed when a polymeric liquid crosslinked by chemical bonds. An important problem in the

theory of rubber elasticity is the calculation of entropy, which essentially is the number of allowed conformations of the chains constituting the rubber. Steric constraints are an important factor influencing such a problem. For a better understanding, let us try to visualize the tube model. Consider a lightly crosslinked rubber which consists of long strands of polymers between crosslinks (Fig 4a). The strand can be placed on a plane and the cross-section of the other can be represented as dots, as shown in Fig 4b. Due to steric constraints, the strand cannot cross the dots, hence the number of conformations becomes much less than in free space. Suppose we assume that the other chains are frozen, then the dots can be regarded as fixed obstacles. One can then see that, the allowed conformation of the strand is confined to a tube-like region, as shown by the dashed lines in Fig 4b. The axis of the tube can be defined as the shortest path connecting the two ends of the strand with the same topology as the strand itself relative to the obstacles. Such a path, which does not violate the steric constraints, is called the primitive path.

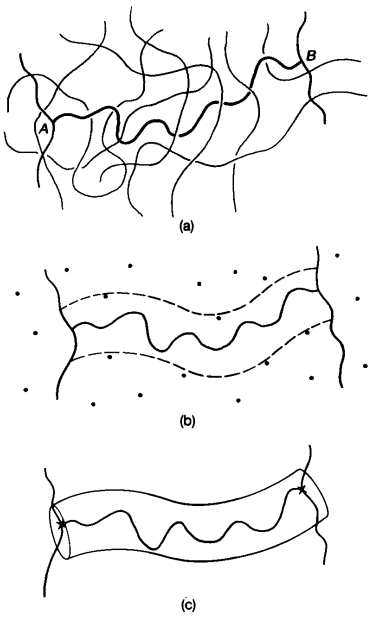

Figure 4: (a) A strand in a rubber. A and B denote the crosslinks, (b) Schematic picture of (a): the strand under consideration is placed on a plane and the other strands intersecting the plane are shown by dots and (c) the tube model. [From ref. 13]

2.2 Reptation Model

Starting from the tube model and considering the motion of the confined chains, Doi and Edwards[13] devised a theory which became well-known as the reptation model. Under the constraints imposed by the tube, the chain motion can thought as being in the direction of the reptation tube. This process leads to the disentangling of the chain. The path of the reptation tube is termed the primitive path, which was explained earlier in the tube model.

Both the actual chain and the primitive path represent random coils and hence display Gaussian scaling. Since the end-to-end distances are equal for the polymer chain and the primitive path,

$$R_0^2 = N_R a_R^2 = l_{pr} a_{pr} \quad \textbf{(5)}$$

where l_{pr} is the contour of the tube/primitive path, a_{pr} is the persistence length of the primitive path which characterizes the stiffness of the primitive path, N_R is the number of Rouse subsections of the chain and a_R the length of each subsection. The process of disentangling in the reptation model is shown in Fig 5. The motion of the chain in the primitive path is described as diffusion along the contour. The associated diffusion coefficient can be derived from the well known Einstein relationship.

$$D' = \frac{kT}{\zeta_p} \quad \textbf{(6)}$$

where D' is the diffusion coefficient for the chain within the tube along the primitive path, and ζ_p is the friction factor for the chain. By definition there are no entanglements within the tube, so

$$\zeta_p = N_R \zeta_R \quad \textbf{(7)}$$

where ζ_R is the friction factor of a chain subsection.

Introducing eq. 7 in eq. 6

$$D' = \frac{kT}{N_R \zeta_R} \qquad \textbf{(8)}$$

The time for the chain to completely diffuse out of the reptation tube is called the "reptation time" τ_d. Such random diffusion is governed by laws for Brownian motion so,

$$\tau_d = \frac{l_{pr}^2}{D'} \qquad \textbf{(9)}$$

Combining this with eq. 5 and eq. 8, we obtain

$$\tau_d = \zeta_R N_R^3 \qquad \textbf{(10)}$$

The reptation model predicts that the relaxation time (and viscosity) scales with the molecular weight to the power 3. As mentioned previously, the power 3.4 is observed experimentally. Thus the reptation model comes close to predicting the right molecular weight dependence.

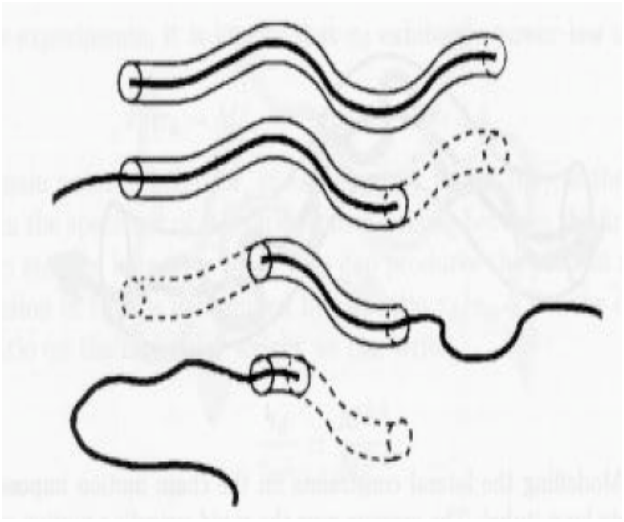

Figure 5: The reptation model. [From ref. 13]

Having discussed the theory of entanglements in polymers, the models mentioned in the introductory chapter are discussed below.

2.3 Binary Contact Model

Fig. 3b illustrates a schematic of the entanglement phenomena. The tortuous path taken by the chain due to presence of surrounding chains can be described by entanglement junctions where two or more chains come into contact with each other. Wu[3] proposed that the binary contacts (two chains come into contact) are much more populous than the higher order ones and hence it is safe to assume that the entanglement junctions consist only of binary contacts. Fig. 6 shows the three different types of binary interchain contacts. The plain contacts are too numerous and occur even at molecular weights lower than M_e and hence are not expected to form entanglement junctions. Thus it is expected that some kind of hooking geometry is then involved in the formation of entanglements. Wu[3] showed that the geometry of binary contact hooking seemed to best describe the formation of entanglement junctions.

The binary contact model[3] identifies the onset of entanglement by a fixed number of binary contacts between Kuhn segments along an entangled length. The number of Kuhn segments per unit volume is[3]

$$c_k = \frac{\rho N_A}{M_0 C_\infty} \qquad \textbf{(11)}$$

where ρ is the polymer density, C_∞ is the characteristic ratio and M_0 is the monomer molecular weight.

The number of binary contacts per unit volume is given by this concentration, multiplied by the probability of finding another Kuhn segment in the immediate neighborhood of the segment. This probability is proportional to $c_K l_K^3$. The number of binary contacts per unit volume is[3]

$$n_b \propto c_k^2 l_k^3 \qquad \textbf{(12)}$$

The number of entangled lengths per unit volume is[3]

$$n_c = \frac{\rho N_A}{M_e} \qquad \textbf{(13)}$$

Using eq. 12 and 13, the number of binary contacts N_{bc} per entangled length is[3]

$$N_{bc} = \frac{\rho N_A}{M_0} \frac{l_k^3}{C_\infty^2} \frac{M_e}{M_0} \qquad \textbf{(14)}$$

The model postulates that N_{bc} will remain a constant for the onset of entanglement irrespective of the species of the polymer.

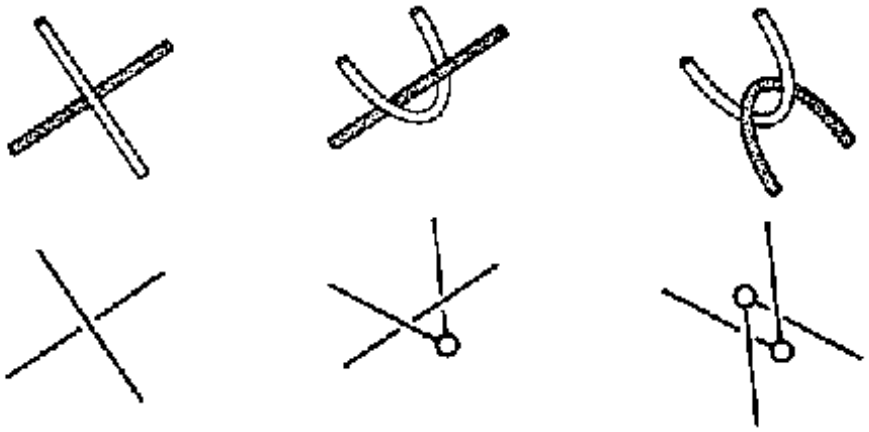

(a) **(b)** **(c)**

Figure 6: Types of interchain contacts- (a) Plain, (b) Single hooking and (c) Binary contact hooking. **[From ref. 3]**

2.4 Packing model

The packing model was first introduced by Witten[14] in modeling the interfacial tension between two immiscible polymers. This model was extended to describe the process of entanglement and various packing models have been proposed in literature.[4-6] In particular, Fetters et al.[4] discuss a packing model to correlate M_e with the degree of entanglement and then with the size of the molecular coils. They introduce a parameter

called the "packing length" p which reflects the degree to which molecules interpenetrate each other's space.

Packing models[4-6] assume that a strand becomes entangled when its ratio of pervaded over occupied volume reaches a critical value. The schematic of the packing model is given in Fig. 7. Motion is unhindered at the segmental level, but as the length of a strand increases, the number of available conformations is increasingly restricted by neighboring chains. The volume occupied by a strand of molecular weight M is

$$V_c = \frac{M}{\rho N_A} \tag{15}$$

The volume pervaded by a molecule, V_{sp}, as that of the smallest sphere that can completely contain a molecule, is proportional to the cube of the root-mean-square radius of gyration R_g, we have

$$V_{sp} = A\left\langle R_g^2 \right\rangle_0^{3/2} \tag{16}$$

where A is a geometrical factor equal to one for flexible polymers.

The measure of the degree of entanglement will be the number N_{sp} of chains of length M that would completely fill the volume V_{sp}. This is the ratio of V_{sp} to V_c.

$$N_{sp} = \frac{V_{sp}}{V_c} = \frac{A\left\langle R_g^2 \right\rangle_0^{3/2} \rho N_A}{M} = A\left(\frac{\left\langle R_g^2 \right\rangle_0}{M} \right)^{3/2} \rho N_A M^{1/2} \tag{17}$$

Fetters et al.[4] proposed that when N_{sp} = 2, there are two chains occupying the space pervaded by each one, and hence this could be used as the criterion for onset of entanglement. The molecular weight at the threshold of entanglement was identified as the entanglement molecular weight M_e which can be expressed as

$$M_e = \left(\frac{\langle R^2 \rangle_0}{M} \right)^{-3} (B\rho N_A)^{-2} = \frac{p^3 \rho N_A}{B^2} \qquad \textbf{(18)}$$

where

$B \equiv \left(\frac{A}{2(6^{3/2})} \right)$, $\langle R^2 \rangle_0 = 6\langle R_g^2 \rangle_0$ and packing length, $p = \frac{V_c}{\langle R^2 \rangle_0} = \frac{M}{\langle R^2 \rangle_0 \rho N_A}$

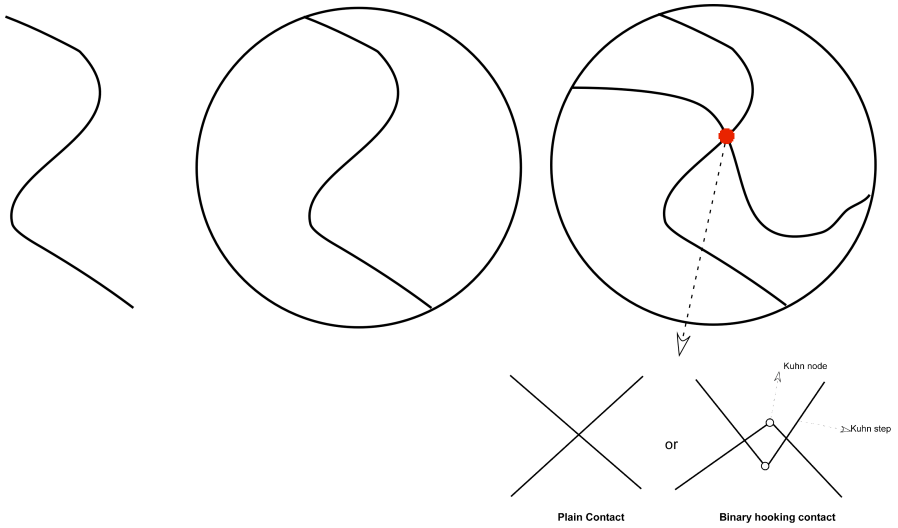

Figure 7: Schematic of the packing model. [Based on ref. 4]

There are some drawbacks to the packing model. Essentially, the assumption that the onset of entanglement is dictated by the ratio $N_{sp} = 2$ is arbitrary. The ratio defines the number of chains occupying the space pervaded by one chain. This would mean that even plain and single-hooking will contribute towards the entanglements (Fig. 7). As explained by Wu[3], plain hooking occurs even in molecular weights below the entanglement molecular weight and thus do not contribute to entanglements. Moreover, unlike the persistence length l_p, the so called "packing length" p defined in this model is not a physical property of the chain that can be measured directly. It is just the ratio of the occupied volume over mean square end-to-end distance and has the dimensions of length, but physically does not represent anything. Essentially, we see that the packing model

overestimates the structural geometry involved in entanglements and hence cannot be used as an appropriate model to treat entanglements.

2.5 Colby and Rubenstein model (Binary contact per pervaded volume model)

Colby et al.[7] combined the binary contact and packing concepts, suggesting that an entanglement is determined by a critical number of binary contacts in the volume pervaded by the entangled reference strand (Fig. 8). This number is obtained by multiplying the number of binary contacts per unit volume (Eq. 12) to the pervaded volume, proportional to $<R_g>^{3/2}$ (Eq. 16) giving,

$$n_v = c_k^2 l_k^3 \left\langle R_g^2 \right\rangle_0^{3/2} \qquad \textbf{(19)}$$

The model postulates that n_v will remain a constant for the onset of entanglement irrespective of the species of the polymer. By combining the concepts of packing model and the binary contact model, the Colby Rubenstein model[7] seems to overcome the inadequacies of the packing model.

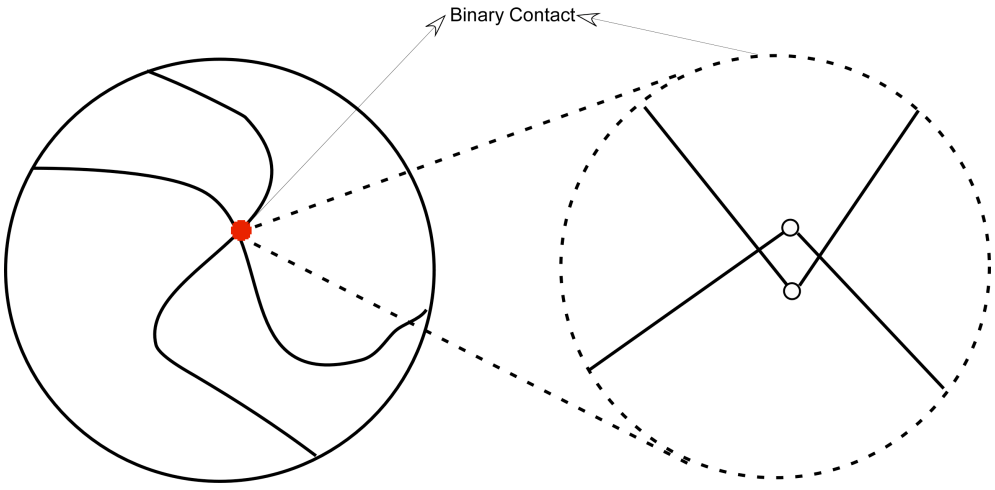

Figure 8: Schematic of the Colby and Rubenstein model. [Based on ref.7]

Having discussed the models that relate chain dimensions like l_p and R_g to M_e, we will review how small angle scattering is utilized to evaluate l_p and R_g simultaneously for branched polymers.

3. Analysis of branching in polymers by small-angle scattering

Local scattering laws like the Guinier's law[15],

$$I(q) = G\exp\left(\frac{-q^2 R_g^2}{3}\right) \quad \textbf{(20)}$$

where $I(q)$ is the scattered intensity, scattering vector $q = 4\pi\sin(\theta/2)/\lambda$, θ is the scattering angle, λ is the wavelength of radiation, R_g is the coil radius of gyration and G is defined as $N_p n_p^2$ where N_p is the number of polymer coils in given volume and n_p is a contrast factor equal to the electron density difference between the polymer coil and the solvent for x-ray scattering; and the power law, describing a mass-fractal object of dimension d_f,[15]

$$I(q) = B_f q^{-d_f} \quad \text{for } 1 \le d_f < 3. \quad \textbf{(21)}$$

where B_f is the power law prefactor, give an account of local features like size and surface/mass scaling.

Studies conducted on fractal analysis of power law behavior in small angle scattering[15] have made it apparent that a number of materials display at least two observable power-law scaling regime. Polymers for example, contain two structural levels, the overall radius of gyration R_g and the substructural persistence length l_p. Polymer melts display Gaussian scaling and show a mass-fractal dimension of 2. For polymer chains in solution that are swollen or slightly collapsed, due to either good or poor solvent conditions, a deviation from a mass-fractal dimension of 2 is expected.

Several studies[15, 16] have observed power-law regimes for such systems, exhibiting structural limits at both high q and low q. These limits are visible as regimes of exponential decay as seen in Fig. 10. This behavior can be interpreted as mass-fractal scattering from a large-scale structure at low q power-law regime and mass-fractal scattering from small-scale substructures in the high q power-law regime. The unified equation described by Beaucage[15] describes a complex morphology over a wide range of q in terms of structural levels. This approach has proven useful in describing mass fractal systems.[17] A major contribution of this approach has been in describing the transition regime between structural levels in small-angle scattering. In the unified approach, small-angle scattering is described by a structurally-limited summation of scattering laws from each level of structure. A level of structure corresponds to a Guinier regime and a structurally limited power-law regime. A power-law of -2 is expected for the Gaussian regime and a power-law of -1 for the persistence regime. To resolve the persistence length, l_p, a log-log plot of $I(q)$ versus q can be made and the two power-law regimes matched with lines of slopes -2 and -1. The intersection of these two lines in q is related to the persistence length through $6/(\pi q_{\text{intersection}}) = l_p$.

Beaucage[11, 17] also applied the unified approach to quantify the branch content by considering aggregates formed from smaller primary particles (Fig. 9). Such a description can be extended to polymers by considering the primary particles to be Kuhn steps. Further, such a structure could be considered to be linear or branched, as shown in Fig. 9. The open circles, p, in Fig. 9b represent the minimum path through the aggregate. A scaling relationship between the degree of aggregation z, the minimum path p, and the overall structural size R_2 and size of the primary particle R_1 can be given as[17],

$$p^c = z = \left(\frac{R_2}{R_1}\right)^{d_f} \tag{22}$$

where c is known as the connectivity dimension, which is equal to 1 for a linear chain and d_f for regular objects. A second scaling relationship between the above terms could be expressed in terms of the minimum dimension d_{min} [17] as,

$$p = \left(\frac{R_2}{R_1}\right)^{d_{\min}}$$
$$c = \frac{d_f}{d_{\min}} \tag{23}$$

where d_{min} represents the mass fractal dimension of the minimum path (Fig. 9b).

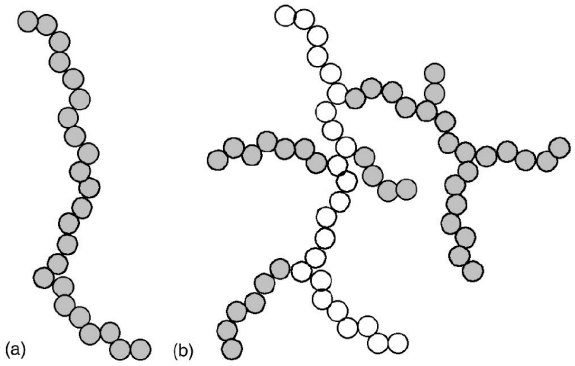

Figure 9. a) Linear aggregate, b) Branched aggregate; composed of primary particles. The open circles in b) represent minimum path, p, through an aggregate. [From ref. 11]

Beaucage[17] showed that one could obtain branch content from eq. 22 and eq. 23 as follows,

$$\phi_{br} = \frac{z - p}{z} = 1 - z^{\frac{1}{c}-1} = 1 - \left(\frac{R_2}{R_1}\right)^{d_{\min} - d_f} \tag{24}$$

The parameter d_{min} could be calculated from the modified power law prefactor equation to account for branched structures and expressing it as,

$$B_f = \frac{G_2 d_{\min}}{R_{g2}^{d_f}} \Gamma\left(\frac{d_f}{2}\right) \qquad \textbf{(25)}$$

where G_2 is the Guinier prefactor for the aggregate, R_{g2} is the aggregate radius of gyration, d_f is the mass fractal dimension and d_{min} is defined in eq. 25. Thus small angle scattering offers a unique tool for simultaneous observation of R_g and l_p of branched structures. The overall size of a polymer is displayed at a lower scattering angle, while the persistence length is observed at high angles as seen in Fig. 10.

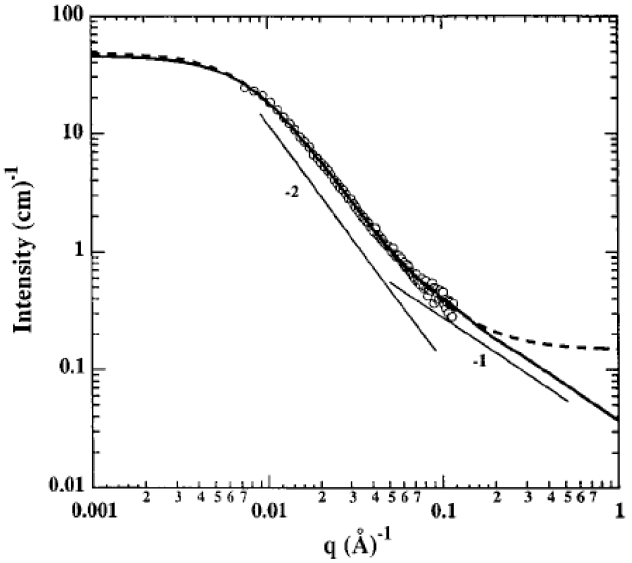

Figure 10: Small-angle scattering data. A power-law of -2 is seen for the Gaussian regime and a power- law of -1 for the persistence regime. [From ref. 16]

Proposed work

The proposed work will focus on evaluating the structural parameters such as persistence length l_p and radius of gyration R_g of a wide range of linear and branched polymers that can be obtained from small-angle neutron scattering experiments. The physical properties such as M_e, M_c and G_N^0 can then be estimated from a suitable model. As discussed earlier, the packing model[4] has some drawbacks in its approach, while the Colby Rubenstein

model[7] seems to overcome the inadequacies of the packing models and is expected to give better estimates of the physical properties.

The model[7] can be used initially for estimating n_v (critical number of binary contacts in the volume pervaded by the entangled reference strand) from rheological data available in literature for linear polymers and chain dimensions that can be measured from small-angle scattering. The estimated n_v can then be used to calculate the physical properties of branched polymers. The results from such an approach can then be verified with data obtained from rheological experiments on branched polymers. The packing model[4] will also be applied to obtain M_e. This would confirm its inadequacy in describing the entanglement behavior correctly. Further, it is intended to correlate the data pertaining to branching in polymers (ϕ_{br}) obtained from neutron scattering studies with these physical properties to gain a better understanding of the effects of branch content on the entanglement behavior of polymers.

References

1. *Effect of short-chain branching on the rheology of polyolefins*. Garcia-Franco, C. A.; Harrington, B. A.; Lohse, D. J. *Macromolecules* **2006,** 39, (7), 2710-2717.
2. *Effect of long-chain branching on the rheology of 1,4-polyisoprene*. Santangelo, P. G.; Roland, C. M. *Journal of Non-Crystalline Solids* **1998,** 235, 709-716.
3. *Chain structure and entanglement*. Wu, S. *Journal of Polymer Science Part B-Polymer Physics* **1989,** 27, (4), 723-741.
4. *Connection between polymer molecular-weight, density, chain dimensions, and melt viscoelastic properties*. Fetters, L. J.; Lohse, D. J.; Richter, D.; Witten, T. A.; Zirkel, A. *Macromolecules* **1994,** 27, (17), 4639-4647.

5. *Number of entanglement strands per cubed tube diameter, a fundamental aspect of topological universality in polymer viscoelasticity*. Lin, Y. H. *Macromolecules* **1987,** 20, (12), 3080-3083.
6. *New view of entanglements in dense polymer systems* Kavassalis, T. A.; Noolandi, J. *Physical Review Letters* **1987,** 59, (23), 2674-2677.
7. *Chain entanglement in polymer melts and solutions*. Colby, R. H.; Rubinstein, M.; Viovy, J. L. *Macromolecules* **1992,** 25, (2), 996-998.
8. *Entanglement interactions in polymers and the chain contour concentration* Graessley, W. W.; Edwards, S. F. *Polymer* **1981,** 22, (10), 1329-1334.
9. *"Intrinsic" and "topological" stiffness in branched polymers.* Connolly, R.; Bellesia, G.; Timoshenko, E. G.; Kuznetsov, Y. A.; Elli, S.; Ganazzoli, F. *Macromolecules* **2005,** 38, (12), 5288-5299.
10. Ramachandran, R.; Beaucage, G.; Kulkarni, A. S. *In preparation*.
11. *Quantification of branching in disordered materials*. Kulkarni, A. S.; Beaucage, G. *Journal of Polymer Science Part B-Polymer Physics* **2006,** 44, (10), 1395-1405.
12. *The viscosity of polymers and their concentrated solutions*. Berry, G. C.; Fox, T. G. *Adv. Polym Sci.* **1967,** 5,261-357.
13. *The Theory of Polymer Dynamics*. Doi, M.; Edwards, S. F. Oxford Science Publications: Oxford, 1986.
14. *Theory of stress distribution in block copolymer microdomains*. Witten, T. A.; Milner, S. T.; Wang, Z.-G., In *Multiphase Macromolecular Systems*, Culbertson, B. M., Ed. Plenum: New York, 1989; 655-663.
15. *Approximations leading to a unified exponential power-law approach to small-angle scattering*. Beaucage, G. *Journal of Applied Crystallography* **1995,** 28, 717-728.

16. *Persistence length of isotactic poly(hydroxy butyrate)*. Beaucage, G.; Rane, S.; Sukumaran, S.; Satkowski, M. M.; Schechtman, L. A.; Doi, Y. *Macromolecules* **1997,** 30, (14), 4158-4162.
17. *Determination of branch fraction and minimum dimension of mass-fractal aggregates.* Beaucage, G. *Physical Review E* **2004,** 70, (3), 10.